Supporting Information

Xu et al. 10.1073/pnas.1718414115

SI Materials and Methods

Mouse Experiments. KP and KPI mice were generated by crossing *LSL-Kras*$^{G12D/+}$; *p53*$^{fl/fl}$ (1, 2) to *Irs1*$^{fl/fl}$; *Irs2*$^{fl/fl}$ (3) mice. Five- to 6-wk-old mice were infected by a single 67.5-μL intranasal instillation of 3×10^7 infectious particles of adenovirus-Cre (University of Iowa), following isoflurane anesthesia (4). In survival studies, mice were killed when they reached moribund stage. For xenograft studies, human NSCLC cells were s.c. injected into the flanks of 6-wk-old female athymic nude mice (Jax; 002019) in 100 μL of RPMI with 15% or 30% phenol red-free, growth factor reduced Matrigel (BD Biosciences). Tumors were measured in live mice twice a week using a digital caliper and tumor volumes were estimated using the formula: $V = (L \times W^2)/2$, where V is the volume, L is the length, and W is the width. Following the killing and tumor harvest, tumor volumes were estimated according to the ellipsoid formula: $4/3 \times \pi \times (a/2 \times b/2 \times c/2)$. Chloroquine (60 mg/kg; Sigma) or vehicle control (PBS) was injected intraperitoneally (5 d a week over 5 wk) into mice when median tumor volume reached ∼150 mm^3.

Tumor Burden Quantification and Grading. For genetically engineered mouse model studies (KP and KPI mice), formalin-fixed lung lobes were bisected, embedded in paraffin, transversely sectioned, and stained with hematoxylin and eosin (H&E). Lung tumor burden was measured in the H&E-stained sections using cellSens software by quantifying total tumor area in each bisected lobe and normalizing it to the corresponding lobe area. Values represent averages of whole-lung tumor burden from at least six mice. Tumor grading was performed by a pathologist in a blinded fashion, using H&E-stained lung sections, based on the following criteria: Grade 1 and 2 tumors are adenomas with nuclei of uniform size and shape. Grade 1 tumors are open and lacy with air spaces between cords of tumor cells. Grade 2 tumors are solid. Grade 3 and 4 tumors are adenocarcinomas with pleiomorphic nuclei that vary in size and shape. Grade 4 tumors show nuclear pleomorphism with invasion of stroma in the spaces around bronchi and blood vessels. Grade 4 tumors metastasize to mediastinal lymph nodes. Mice harboring only grade 1 and 2 lung tumors were categorized as having "low-grade" tumors; those harboring grade 2 and grade 3 tumors, "medium grade," and those with grade 3 and grade 4 tumors, "high grade." At moribund stage (Fig. 1*H*), all mice harbored either medium- or high-grade tumors.

MRI. MRI experiments were carried out with a Bruker 7-T 30-cm scanner, equipped with a 450 mT/m gradient system (Bruker-Biospin). The ^{1}H Larmor frequency was 300.3 MHz. Animals were anesthetized by inhalation of isoflurane, initially at 2–3% and maintained at 1.0–2.5%, through a nose cone for the duration of the scanning. Mice were placed on a Bruker cardiac array receive-only probe mounted to the scanner animal table, and moved inside an 86-mm Bruker transmit-only resonator and the bore of the scanner. Respiration rates were monitored and observed in a range of 25–70 per minute throughout the scanning. Black blood magnetic resonance images were acquired with a Bruker IntraGate Flash sequence, a retrospective imaging method utilizing additional navigator signals for image reconstruction and eliminating motion artifact without physically using ECG or respiration gating. The following parameters were used: field of view, 30 mm × 18 mm; matrix, 256 × 256; echo time, 2.112 ms; repetition time, 45.211 ms; number of repetitions, 100 (from which 10 cardiac frames were reconstructed for each slice). Ten to 12 1-mm-thick consecutive axial slices were acquired for each mouse with an acquisition time of 20 min. Digital Imaging and Communications in Medicine files of the MRI images were loaded into 3D Slicer software for tumor volume quantification. Tumor volume was assessed by the sum of all identified tumor areas in 30 consecutive frames for each mouse.

Tumor Dissociation and Cell Culture. Tumors from moribund KP and KPI mice were dissociated in calcium/magnesium-free HBSS (Invitrogen) containing 0.025% trypsin-EDTA (Invitrogen) and 1 mg/mL collagenase IV (Worthington Biochemicals). Following a 2-h incubation with rotation at 37 °C, the samples were triturated and centrifuged. The resulting pellets were resuspended in culture medium and filtered through 40-μm cell strainers (BD Falcon) before in vitro culture. Human NSCLC cell lines A549 and Calu-1 were obtained from the American Type Culture Collection (ATCC). ATCC cell lines are routinely authenticated by STR profiling. All cells were cultured in RPMI supplemented with 10% FBS.

Cell Line Genotyping. KP and KPI cells were trypsinized, washed twice in ice-cold PBS, and incubated overnight at 50 °C in digestion buffer containing 100 mM NaCl, 10 mM Tris·Cl, pH 8, 25 mM EDTA, pH 8, 0.5% SDS, and 0.1 mg/mL proteinase K. Samples were extracted with an equal volume of phenol, chloroform, and isoamyl alcohol and centrifuged. Aqueous top layer was transferred to a new tube and DNA was precipitated with 1:10 vol of 3 M sodium acetate and 2 vol of 100% ethanol. Primers and protocols used for genotyping are listed below: *Kras* F1, 5′-GTCTTTCCCCAGCACAGTGC-3′; *Kras*-R1, 5′-CTCTTGCCTACGCCACCAGCTC-3′, *Kras*-SD5, 5′-AGCTAGC-CACCATGGCTTGAGTAAGTCTGCA-3′. *Kras*-F1 and *Kras*-R1 detect wild-type and recombined *Kras* alleles, yielding products that are 622 and 650 bp, respectively. *Kras*-R1 and *Kras*-SD5 detect floxed *Kras* allele, yielding a product that is 500 bp. Genotyping protocol for *Kras* (1): 2 min at 95 °C for initial denaturation; 30 cycles of 30 s at 95 °C, 30 s at 59.2 °C, and 50 s at 72 °C; 10 min at 72 °C for final extension. *Tp53*-A, 5′-CACAAAAACAGGTTAAACCCAG-3′; *Tp53*-B, 5′-AGCACATAGGAGGCAGAGAC-3′; *Tp53*-C, 5′-GAAGACAGAAAAGGGGAGGG-3′. *Tp53*-A and *Tp53*-B detect wild-type and floxed *Tp53* alleles, yielding products that are 288 and 370 bp, respectively. *Tp53*-A and *Tp53*-C detect recombined *Tp53* allele, yielding a product that is 612 bp. Genotyping protocol for *Tp53* (2): 2 min at 94 °C for initial denaturation; 29 cycles of 30 s at 94 °C, 30 s at 58 °C, and 50 s at 72 °C; 5 min at 72 °C for final extension. *Irs1*-Nhe7, 5′-GCTAATAGTGCCAGGTGTGA-GATC-3′; *Irs1*-Nhe10, 5′-GGACGCGGGTGACCTGCTAG-3′; *Irs1*-UTRRev1, 5′-AGAGAGAAGCCCTTCTGTGGCTGCTCC-AAACACA-3′. *Irs1*-Nhe7 and *Irs1*-Nhe10 detect wild-type and floxed *Irs1* alleles, yielding products that are 278 and 322 bp, respectively. *Irs1*-Nhe7 and *Irs1*-UTRRev1 detect recombined *Irs1* allele, yielding a product that is 589 bp. Genotyping protocol for *Irs1*: 2 min at 95 °C for initial denaturation; 35 cycles of 30 s at 94 °C, 20 s at 64 °C, and 45 s at 72 °C; 10 min at 72 °C for final extension. *Irs2*-5p outer forward, 5′-TCCGATCATATTCAATAACCCTTA-3′; *Irs2*-inner forward, 5′-ACGTCGTCGCCACAGTTCAGAG-3′; *Irs2*-3p outer reverse, 5′-TACACTGAGACAGAAGGTTAGG-3′. *Irs2*-inner forward and *Irs2*-3p outer reverse detect wild-type and floxed *Irs2* alleles, yielding products that are 716 and 750 bp, respectively. *Irs2*-5p outer forward and *Irs2*-3p outer reverse detect recombined *Irs2* allele, yielding a product that is 250 bp. Genotyping protocol for *Irs2* (5) was as follows: 2 min at 95 °C for initial denaturation; 35 cycles of 30 s at 94 °C, 20 s at 60 °C, and 45 s at 72 °C; 10 min at 72 °C for final extension.

Generation of Cells with Stable Gene Knockout, Knockdown, or Overexpression. For generation of human *IR*, *IGF1R*, *IRS1* and *IRS2*, or mouse *Irs1* and *Irs2* stable knockdown lung cancer cells, lentiviral supernatants produced from pLKO plasmids each encoding the corresponding hairpins were used, and infected cells were selected for at least 7 d with either puromycin (4 μg/mL, pLKO.1 plasmids with human *IR*, *IGF1R* hairpins or their control *Scramble* hairpin; pLKO.1 plasmids with *IRS2* hairpin or its control *GFP* hairpin; pLKO.TRC005 plasmids with mouse *Irs1* or *Irs2* hairpin) and/or blasticidin (10–20 μg/mL; pLKO.TRC016 with human *IRS1* hairpin or its control *Scramble* hairpin). Mouse *Irs1* hairpins: sh*Irs1*-1 (TACCGCAACTGCCGAAGATTC) and sh*Irs1*-2 (CGGAACAATTAGTGTGCATAA). Mouse *Irs*2 hairpins: s*hIrs2*-1 (TCATGTCCCTTGACGAGTATG) and sh*Irs2*-2 (TCTCCACTC-TCTGACTATATG); human *IR* hairpins: sh*IR*-1 (GCTCTGTTAC-TTGGCCACTAT) and sh*IR*-2 (AGAGACATCTATGAAACGG-AT); human IGF1R hairpins: sh*IGF1R*-1 (GCCGAAGATTTCA-CAGTCAAA) and sh*IGF1R*-2 (CCTT-GGACGTTCTTTCAGCAT); human *IRS1* hairpins: sh*IRS1*-1 (ACTCATTGCCAAGATCCTTTA) and sh*IRS1*-2 (GGGTTTGGAGAATGGTCTTAA); human *IRS2* hairpins: sh*IRS2*-1 (TCTCCGCTCTCCGACTACATG); sh*IRS2*-2 (GTGAAGATCTGTCTGGCTTTA); sh*IRS2-3* (CCCAGAGG-ACTACGGAGACAT) and control *GFP* hairpins: sh*GFP* (CTAC-AACAGCCACAACGTCCT and TCTCGGCATGGACGAGCTGTA); control *Scramble* hairpin: sh*Scr* (CCTAAGGTTAAG-TCGCCC-TCG). A549 DKD and Calu-1 DKD-1 cells were infected with sh*IRS1*-1 and sh*IRS2*-1; Calu-1 DKD-2 cells were infected with sh*IRS1*-1 and sh*IRS2*-2. For generation of A549 *IRS1* and *IRS2* DKO cells, single targeting guide RNAs were cloned into the empty backbone construct pSpCas9(BB)-2A-Puro. Empty pSpCas9(BB)-2A-Puro plasmid was used as negative control. Lentiviral supernatants were produced, and cells were infected and selected for at least 7 d with puromycin (4 μg/mL). Human *IRS1*-targeting guide RNA: forward, 5′-GGCTTCTCGGACGTGCGCA-3′; reverse, 5′-TGCGCACG-TCCGAGAAGCC-3′. Human *IRS2*-targeting guide RNA: forward, 5′-ACCACAGCGTGCGCAAGTG-3′; reverse, 5′-CACTTGCG-CACGCTGTGGT-3′. Individual clones that survived selection were validated via QPCR and Western blot. A single *IRS1* and *IRS2* DKO clone was expanded and used for subsequent experiments. For GFP-LC3 expression, cells were lentivirally infected with pBABEpuro GFP-LC3 (22405; Addgene) and selected with puromycin as described above.

Cell Proliferation Assay. The assay was performed using XTT Cell Viability Kit (Cell Signaling Technology) according to the manufacturer's protocol. Eight hundred cells were plated per well in 96-well plates 1 d before subjecting them to treatment conditions, as described in the figure legends.

GFP-LC3 Expression and Punctae Quantification. Cells stably expressing GFP-LC3 were seeded on cover glasses (1943-10025; Bellco Glass) in six-well plates in media with 10% serum, with or without chloroquine treatment (10 μM) for the indicated periods of time. After media removal, the cells were washed three times with ice-cold PBS and fixed in 4% EM-grade paraformaldehyde (catalog no. 15710; VWR) in PBS for 30 min at room temperature. Cells were then stained with 1 μg/mL DAPI (catalog no. D3571; Thermo Scientific) in PBS for 15 min at room temperature. Cells were then rinsed five times with PBS before being mounted on glass slides (catalog no. 48311-703; VWR) with Fluoroshield (catalog no. F6182; Sigma). Image acquisition was performed using a Nikon Eclipse 90i Advanced Automated Research Microscope equipped with a standard optical filter set including DAPI and FITC. Images were captured with a 60× objective and the NIS-Elements Advanced Research Microscope Imaging Software (Nikon). Exposure time for DAPI acquisition was 20 ms and that for FITC acquisition was 200 ms. For each condition and each cell line, 15–20 representative images were captured and used for quantification. The total number of cells as well as the number of cells positive for GFP-LC3 punctae were visually counted. The data represent averages of three independent experiments.

Reverse-Phase Protein Array. Cells were rinsed twice with ice-cold PBS and collected in lysis buffer containing 1% Triton X-100, 50 mM Hepes, pH 7.4, 150 mM NaCl, 1.5 mM $MgCl_2$, 1 mM EGTA, 100 mM NaF, 10 mM Na pyrophosphate, 1 mM Na_3VO_4, 10% glycerol, and protease and phosphatase inhibitors (Roche). Protein lysates were shipped to the RPPA Core Facility at University of Texas MD Anderson Cancer Center where reverse-phase protein array (RPPA) was performed as previously described (6).

Immunoblotting. Cells were rinsed once with ice-cold PBS and collected in lysis buffer containing 50 mM Hepes, pH 7.4, 40 mM NaCl, 2 mM EDTA, 50 mM NaF, 10 mM sodium pyrophosphate, 10 mM sodium β-glycerophosphate, EDTA-free protease inhibitors (Roche), and 1% Triton X-100. Proteins were resolved by 6–15% SDS/PAGE and transferred to PVDF membrane (Merck Millipore). Membranes were blocked with 5% nonfat dry milk in PBS with Tween (PBS-T) and then incubated with primary antibody overnight at 4 °C. Following PBS-T washing, membranes were incubated with peroxidase-conjugated secondary antibody for 1 h at room temperature and exposed on film using Enhanced Chemiluminescence Detection System (Thermo Scientific). Antibodies were from Abcam: SLC7A1 (1:1,000, ab37588); Cell Signaling Technology: AKT (1:2,000; CST; 4691), AKT pS473 (1:2,000; CST; 4058), AKT pT308 (1:1,000; CST; 4056), ERK (1:5,000; CST; 4695), ERK pT202/Y204 (1:1,000; CST; 4376), GSK3β (1:1,000; CST; 9315), GSK3β pS9 (1:1,000; CST; 9322), IGF1R (1:1,000; CST; 9750), IRβ (1:1,000; CST; 3025), LC3B (1:2,000; CST; 2775), IGF1-Rβ pY1135/1136/IRβ pY1150/1151 (1:1,000; CST; 3024), S6 (1:2,000; CST; 2217), S6 pS235/236 (1:1,000; CST; 2211), S6Kα pT389 (1:1,000; CST; 9205), SLC3A2 (1:1,000; CST; 13180), SLC7A5 (1:1,000; CST; 5347), TSC2 (1:1,000; CST; 4308), TSC2 pT1462 (1:1,000; CST; 3617); Santa Cruz Biotechnology: β-actin (1:20,000; sc-47778), GAPDH (1:5,000; sc-25778), and S6Kα (1:1,000; sc-230). Antibodies for Western blot detection of IRS1 and IRS2 (1:1,000) were a gift from M.F.W. IRS1 was detected using a protein G-purified mouse monoclonal antibody raised against residues surrounding S439 of mouse Irs1 (7). IRS2 was detected using a protein G-purified rabbit monoclonal antibody raised against a His-tagged protein containing residues 818–1323 of mouse Irs2.

Luminex Assay. The IRS1 capture antibody (rabbit monoclonal clone 58-10C-31; 05-784R; Millipore) was coupled to magnetic carboxylated microspheres (Luminex Magplex-C beads) as described (8). Antibodies used for the detection of captured IRS1 and associated p110α were biotinylated using reagents from Thermo Fisher (EZ-Link NHS-PEG4-Biotin kit; catalog no. 21330) following the manufacturer's guidelines and keeping the antibody concentrations between 1.5 and 2.0 mg/mL. The antibody used for detection of IRS1 was from Millipore (mouse monoclonal; catalog no. 05-1085) and that for p110α was from Cell Signaling Technology (rabbit monoclonal clone C73F8; CST; 4249). KP and KPI cells were treated with indicated conditions before protein lysates were collected as described in *Immunoblotting*. Protein lysates (60 μg) were incubated with Irs1 capture beads (2,500 beads per well) in a total volume of 50 μL per well of Milliplex MAP Assay Buffer 2 (43-041; Millipore) in 96-well plates, and the assay was performed as described (8). Fluorescence signals from captured Irs1 and p110α were read by a Luminex FlexMap 3D instrument. Median fluorescence intensities (MFIs) were reported by the instrument. The degree of interaction between p110α and Irs1 was measured as the ratio of

MFI of p110α over MFI of Irs1. Triplicates were used per condition for each cell line.

Metabolite Extraction and Quantification. For intracellular metabolite analyses, cells were rinsed once with ice-cold 0.9% NaCl and placed on dry ice. Metabolites were extracted with extraction solution (80% methanol containing a mixture of internal amino acid standards at 90.9 nM each), vortexed for 10 min at 4 °C, and centrifuged at top speed (10 min, 10,000 × *g*, 4 °C). Supernatants were then transferred to fresh Eppendorf tubes and dried with Speedvac. Dried extracts were suspended in 100 μL of water and centrifuged at top speed for 10 min, and the supernatant was analyzed using LC/MS. For media metabolite analyses, metabolites were extracted by combining 10 μL of media with 90 μL of extraction solution, followed by centrifugation and analysis of the supernatant by LC-MS. For Figs. 2*D* and 3*C* and Fig. S5*A*, LC-MS analysis was performed as previously described (9). For Figs. 2*E* and 5 *B* and *D*, data were acquired using a hydrophilic interaction liquid chromatography method with positive-ion mode mass spectrometry (MS) operated on Nexera ×2 UHPLC (Shimadzu Scientific Instruments) coupled to a Q Exactive orbitrap mass spectrometer (Thermo Fisher Scientific) as described (10). For Fig. 2 *C* and *D*, data representing raw peak areas normalized to internal standards were uploaded to Metaboanalyst 3.0 (11), median-normalized, log-transformed, mean-centered, and divided by the SD of each variable.

Statistical Analyses. Data are presented as mean ± SD or ±SEM, unless otherwise indicated. A log-rank test was used for analysis of survival curves, and a nonparametric two-tailed Fisher's exact test was used for analysis of tumor grade. For all other data, when comparing two groups, a two-tailed nonpaired Student *t* test was conducted. For three or more groups, one-way ANOVA was conducted except for growth curves (i.e., in vitro proliferation and in vivo tumor growth), where two-way ANOVA was conducted. In either case, ANOVA was followed by post hoc Tukey's multiple-comparison test. $P < 0.05$ was considered statistically significant.

1. Jackson EL, et al. (2001) Analysis of lung tumor initiation and progression using conditional expression of oncogenic K-ras. *Genes Dev* 15:3243–3248.
2. Jonkers J, et al. (2001) Synergistic tumor suppressor activity of BRCA2 and p53 in a conditional mouse model for breast cancer. *Nat Genet* 29:418–425.
3. Dong X, et al. (2006) Irs1 and Irs2 signaling is essential for hepatic glucose homeostasis and systemic growth. *J Clin Invest* 116:101–114.
4. DuPage M, Dooley AL, Jacks T (2009) Conditional mouse lung cancer models using adenoviral or lentiviral delivery of Cre recombinase. *Nat Protoc* 4:1064–1072.
5. Lin X, et al. (2004) Dysregulation of insulin receptor substrate 2 in beta cells and brain causes obesity and diabetes. *J Clin Invest* 114:908–916.
6. Hennessy BT, et al. (2010) A technical assessment of the utility of reverse phase protein arrays for the study of the functional proteome in non-microdissected human breast cancers. *Clin Proteomics* 6:129–151.
7. Hançer NJ, et al. (2014) Insulin and metabolic stress stimulate multisite serine/threonine phosphorylation of insulin receptor substrate 1 and inhibit tyrosine phosphorylation. *J Biol Chem* 289:12467–12484.
8. Copps KD, Hançer NJ, Qiu W, White MF (2016) Serine 302 phosphorylation of mouse insulin receptor substrate 1 (IRS1) is dispensable for normal insulin signaling and feedback regulation by hepatic S6 kinase. *J Biol Chem* 291: 8602–8617.
9. Birsoy K, et al. (2015) An essential role of the mitochondrial electron transport chain in cell proliferation is to enable aspartate synthesis. *Cell* 162:540–551.
10. Townsend MK, et al. (2013) Reproducibility of metabolomic profiles among men and women in 2 large cohort studies. *Clin Chem* 59:1657–1667.
11. Xia J, Wishart DS (2016) Using MetaboAnalyst 3.0 for comprehensive metabolomics data analysis. *Curr Protoc Bioinformatics* 55:14.10.1–14.10.91.

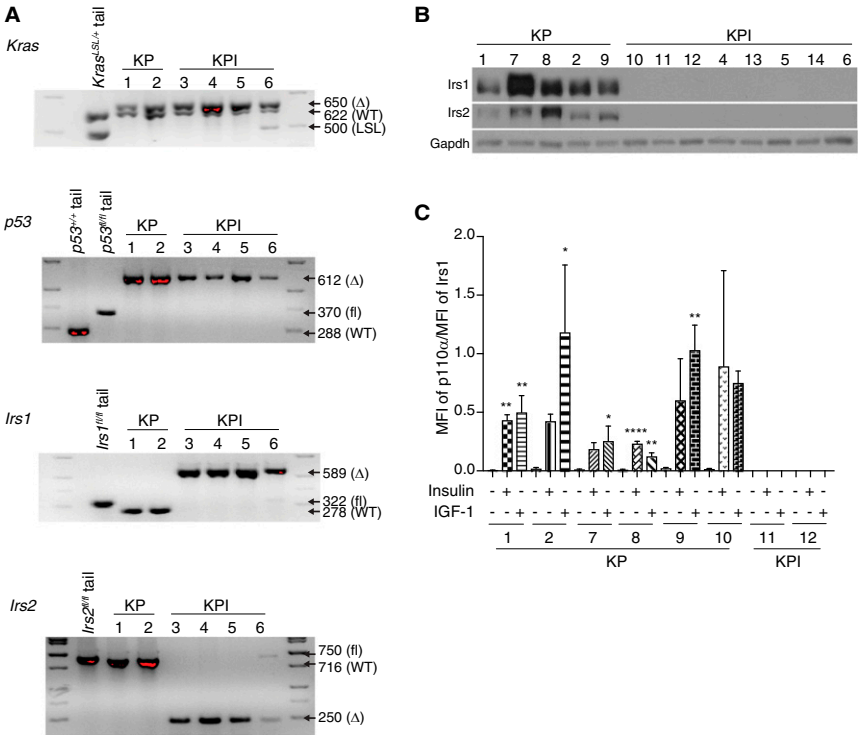

Fig. S1. KPI but not KP cells demonstrate loss of *Irs1*/*Irs2* expression and loss of insulin/IGF1 signaling to Pi3k. (*A*) Genotyping DNA gels showing recombined LSL-*Kras*^{G12D} and *p53*$^{fl/fl}$ alleles in KP (1, 2) and KPI (3–6) cells, in addition to recombined *Irs1*$^{fl/fl}$ and *Irs2*$^{fl/fl}$ alleles in KPI, but not KP cells. KPI-6 shows presence of residual nontransformed cells at this earlier passage, evident by trace levels of nonrecombined LSL-*Kras*^{G12D}, *Irs1*, and *Irs2* alleles. Tail DNA was used as a control for wild-type and floxed alleles. (*B*) Levels of Irs1and Irs2 proteins in five KP (-1, -7, -8, -2, -9) and eight KPI (-10, -11, -12, -4, -13, -5, -14, -6) cell lines; Gapdh was used as a loading control. (*C*) Luminex bead-based assay demonstrating Irs1–Pi3k p110α interaction in KP but not KPI cells. Cells were starved of serum for 1 h and stimulated with insulin (500 ng/mL) or IGF1 (50 ng/mL) for 10 min. Irs1–p110α interaction was quantified as median fluorescence intensity (MFI) of p110α over MFI of Irs1; data indicate the mean ± SD and are representative of three independent experiments; $n = 3$ biological replicates per condition per cell line. *$P < 0.05$, **$P < 0.01$, and ****$P < 0.0001$.

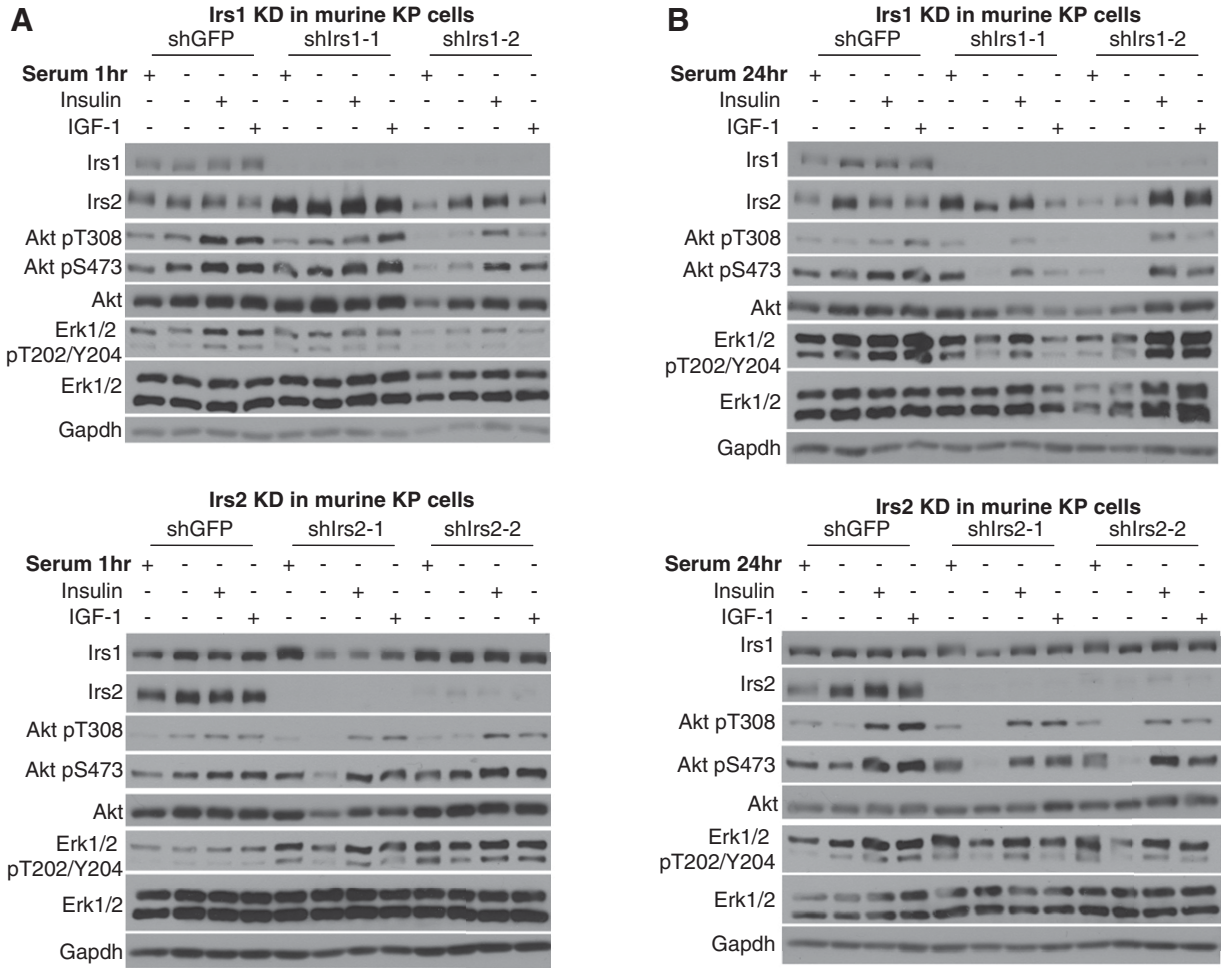

Fig. S2. Single knockdown of *Irs1* or *Irs2* does not suppress Akt signaling in murine *Kras*-mutant lung cancer cells. (*A* and *B*) Levels of Irs1, Irs2, total or phosphorylated Akt and Erk1/2 in murine *p53*-null, *Kras*-mutant lung cancer cells (KP cells) with control *GFP* knockdown or single knockdown of *Irs1* (*Top*) or *Irs2* (*Bottom*). Cells were starved of serum for 1 h (*A*) or 24 h (*B*) and stimulated with insulin (1 μg/mL) or IGF1 (100 ng/mL) for 10 min. Gapdh was used as a loading control.

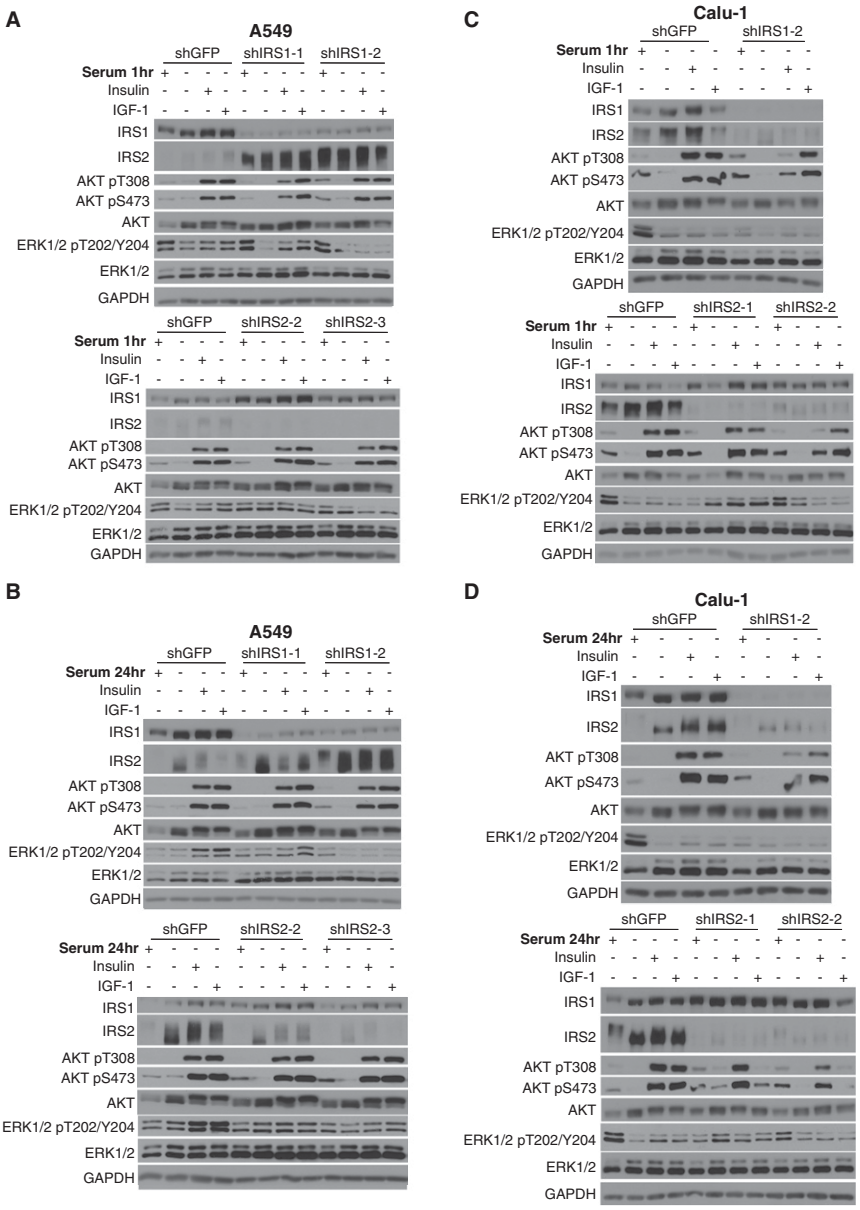

Fig. S3. Single knockdown of *IRS1* or *IRS2* does not suppress AKT signaling in human *KRAS*-mutant NSCLC cells. (*A*–*D*) Levels of IRS1, IRS2, total or phosphorylated AKT and ERK1/2 in *KRAS*-mutant NSCLC A549 (*A* and *B*) and Calu-1 (*C* and *D*) cells with control *GFP* knockdown or single knockdown of *IRS1* (*Top*) or *IRS2* (*Bottom*). Cells were starved of serum for 1 h in *A* and *C*, and 24 h in *B* and *D*, and stimulated with insulin (1 μg/mL for A549 cells, 100 ng/mL for Calu-1 cells) or IGF1 (100 ng/mL for A549 cells, 10 ng/mL for Calu-1 cells) for 10 min. GAPDH was used as a loading control.

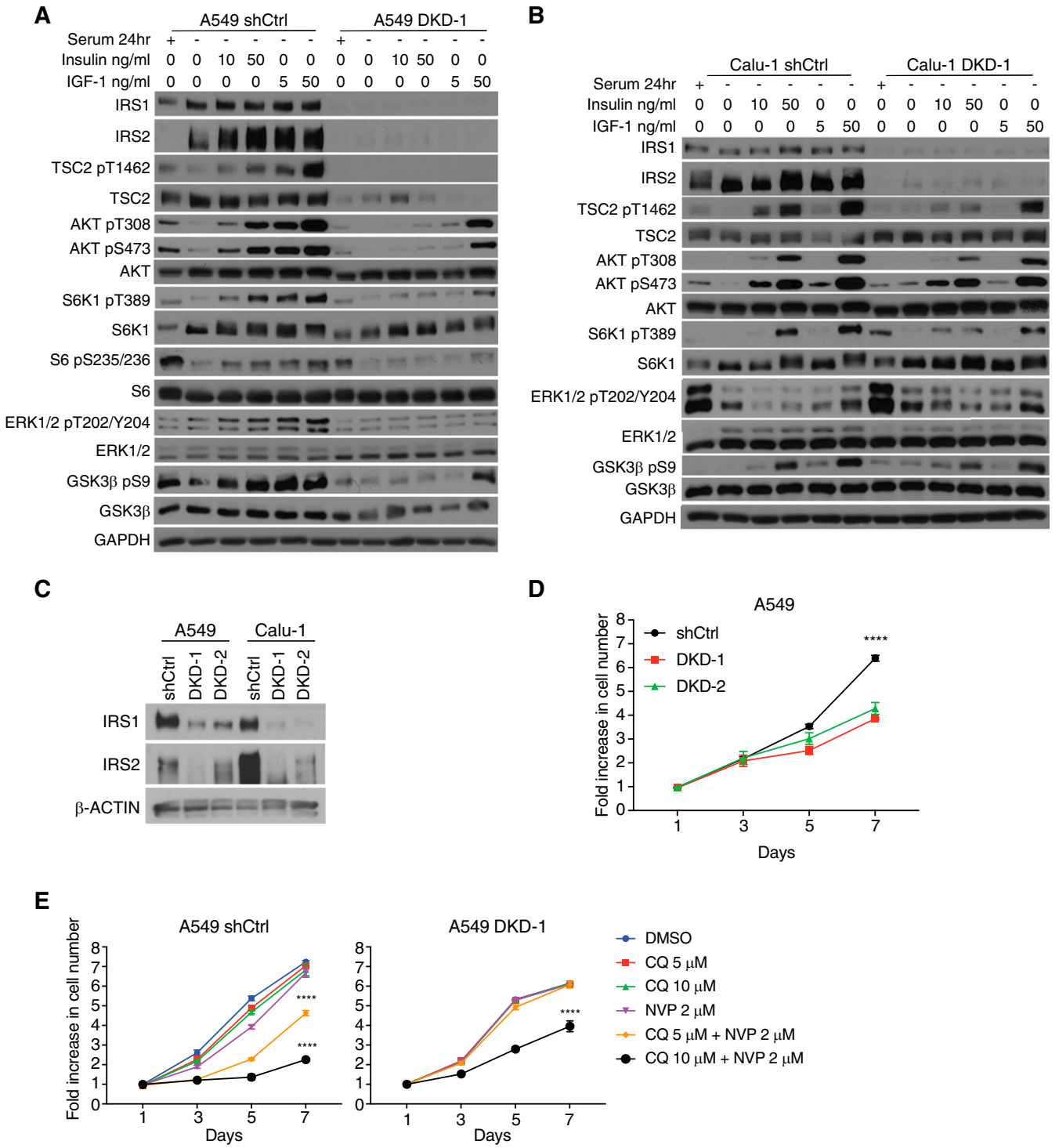

Fig. S4. Concomitant silencing of *IRS1* and *IRS2* in human NSCLC cells impairs insulin/IGF1-stimulated AKT signaling. (*A* and *B*) Levels of IRS1, IRS2, total or phosphorylated ERK1/2, S6K, S6, AKT and its targets TSC-2 and GSK3β in A549 (*A*) or Calu-1 (*B*) cells with control knockdown (sh*GFP*/sh*Scramble*, termed shCtrl) or *IRS1*/*IRS2* double knockdown (DKD). Cells were serum-starved for 24 h and then stimulated with insulin or IGF1 for 10 min. (*C*) Western blots confirming concomitant knockdown of *IRS1* and *IRS2* in A549 and Calu-1 cells using two distinct pairs of hairpins for *IRS1* and *IRS2* (DKD-1 and DKD-2). In *A*–*C*, GAPDH and β-ACTIN were used as loading controls. (*D*) Proliferation curves of A549 shCtrl and DKD cells that were grown under low serum conditions (0.5% serum) over 7 d; $n = 4$. Data represent the mean ± SEM. ****$P < 0.0001$ between shCtrl and DKD conditions. (*E*) Proliferation curves of Calu-1 shCtrl and DKD cells, which were grown in 10% serum and treated with either vehicle control (DMSO), CQ, NVP-AEW541, or both for 7 d; $n = 4$. Data represent the mean ± SEM. ****$P <$ 0.0001 between combinatorial treatment conditions and all other conditions (for A549 shCtrl) or between CQ (10 μM) plus NVP (2 μM) condition and all other conditions (for A549 DKD-1).

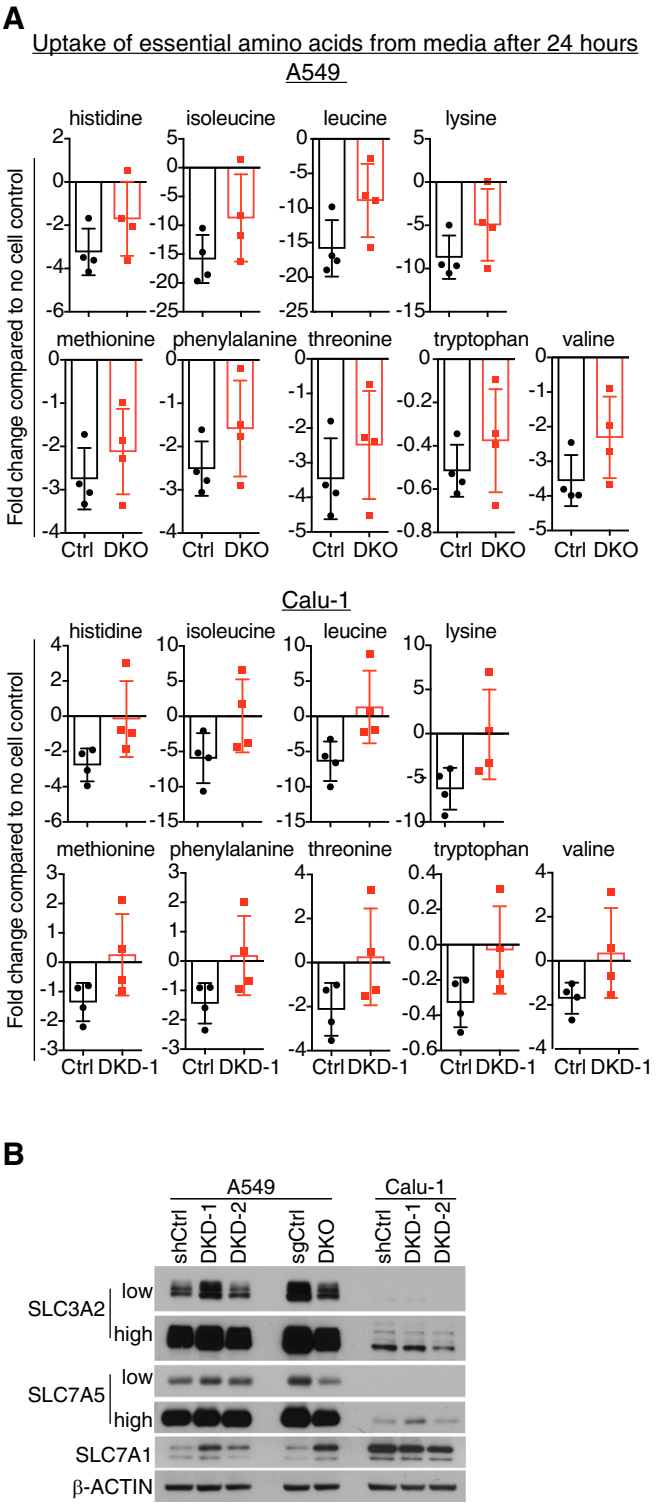

Fig. S5. Concomitant knockdown of *IRS1* and *IRS2* in human NSCLC cells results in decreased uptake of essential amino acids. (*A*) Fold changes in the levels of essential amino acids in media following 24-h incubation with A549 or Calu-1 cells relative to control media incubated in the absence of cells. Compared with their respective control cells, A549 DKO and Calu-1 DKD cells demonstrate a decrease in amino acid uptake from the media; $n = 4$. Data represent the mean ± SD. (*B*) Protein levels of SLC3A2, SLC7A5 (LAT-1), and SLC7A1 (CAT-1) transporters are not consistently altered in NSCLC cells with silencing of *IRS1* and *IRS2*. β-ACTIN was used as a loading control.

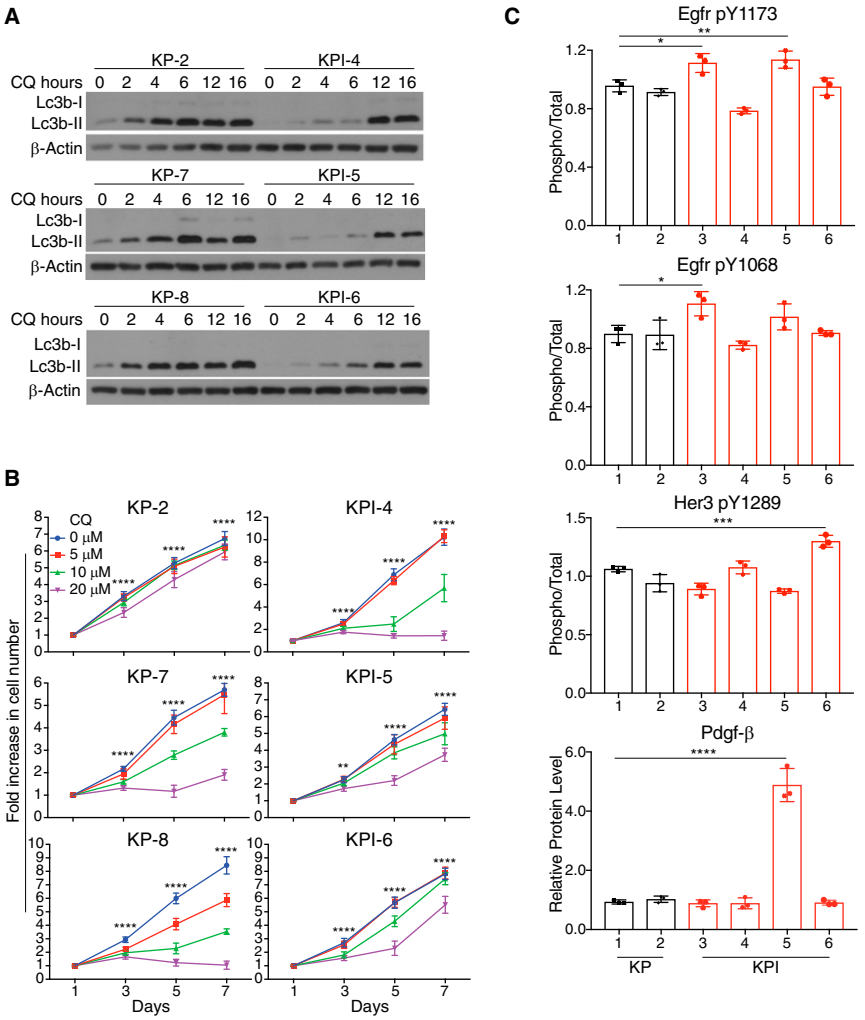

Fig. S6. Murine *Kras*-mutant KPI lung cancer cells with *Irs1*/*Irs2* loss display compensatory induction of alternative receptor tyrosine kinases. (*A*) Levels of Lc3b-I and Lc3b-II in *Kras*-mutant lung cancer cells with *Irs1*/*Irs2* loss (KPI cells) compared with control KP cells with wild-type *Irs1*/*Irs2*. Cells were cultured in the presence of 10% serum and 10 μM chloroquine (CQ) for 0–16 h. Compared with KP cells, KPI cells have reduced Lc3b-II accumulation, indicating decreased autophagic flux. β-Actin was used as a loading control. (*B*) Proliferation curves of KP and KPI cells treated with CQ (0, 5, 10, or 20 μM); $n = 6$; $^{**}P < 0.01$ and $^{****}P < 0.0001$ between 0 and 20 μM conditions. (*C*) Levels of phosphorylated Egfr (pY1173, pY1068), Her3 (pY1289), and total Pdgf-β, as measured by reverse-phase protein array (RPPA) in 1-h serum-starved KP and KPI cell lines. Levels of phosphorylated proteins were normalized to total levels of the respective proteins; $n = 3$ biological replicates; $^{*}P < 0.05$, $^{**}P < 0.01$, $^{***}P < 0.001$, and $^{****}P < 0.0001$. In *B* and *C*, data represent the mean ± SD.

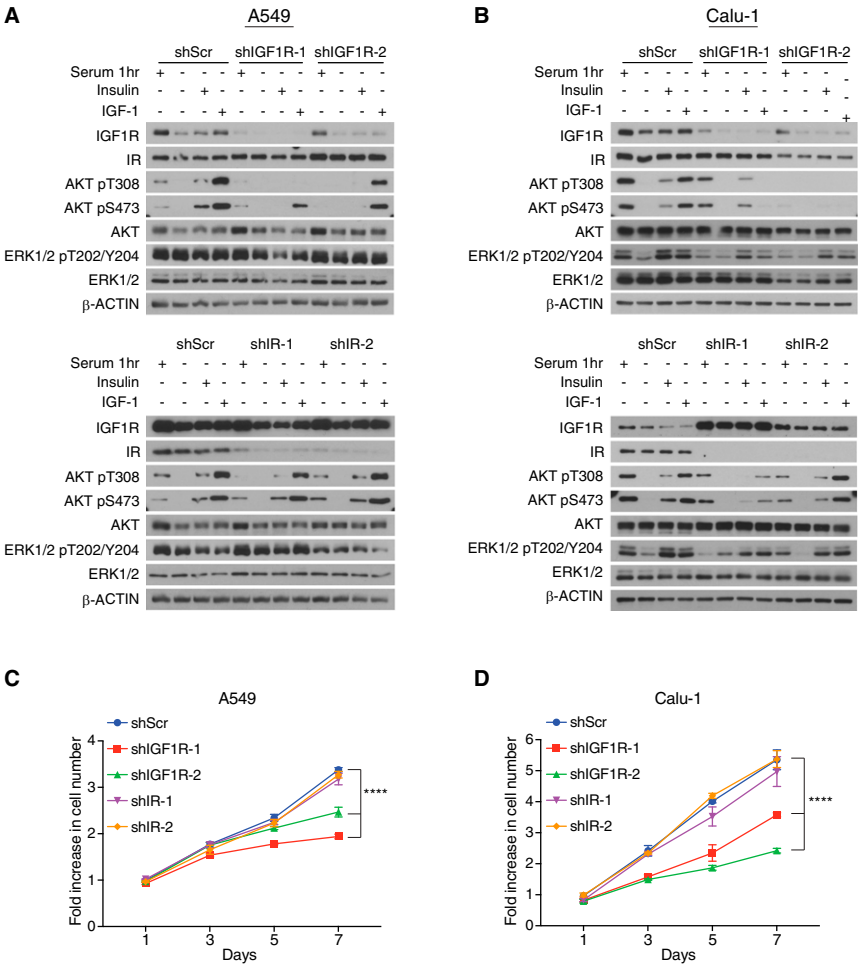

Fig. S7. IGF1 receptors dominate over insulin receptors in transducing insulin/IGF1 signaling and promoting proliferation in human *KRAS*-mutant NSCLC cells. (*A* and *B*) Levels of IGF1R, IR, total or phosphorylated AKT and ERK1/2 in *KRAS*-mutant NSCLC A549 (*A*) or Calu-1 (*B*) cells with control *Scramble* or single knockdown of *IGF1R* (*Top*) or *IR* (*Bottom*). Cells were starved of serum for 1 h and stimulated with insulin (1 μg/mL for A549 cells, 100 ng/mL for Calu-1 cells) or IGF1 (100 ng/mL for A549 cells, 10 ng/mL for Calu-1 cells) for 10 min. β-ACTIN was used as a loading control. (*C* and *D*) Proliferation curves of A549 (*C*) or Calu-1 (*D*) cells with *IGF1R*, *IR*, or control *Scramble* knockdown cultured in low serum (0.1% serum for A549 and 2% serum for Calu-1) over 7 d; $n = 4$. ****$P <$ 0.0001 between shIGF1R and shScr and also between shIGF1R and shIR.

Dataset S1. Reverse-phase protein array (RPPA) data

Dataset S1

List of relative abundance of total proteins and phosphoproteins in KP cells (cell lines 1 and 2) and KPI cells (lines 3–6). Cells were either non-serum starved (10% FBS), serum starved (0% FBS) for 1 h, or serum starved for 1 h and stimulated with 50 ng/mL IGF1 for 10 min (indicated as IGF1). Rows indicate the specific cell line and treatment. Columns indicate the levels of the specific protein/phosphoprotein. All values are normalized for protein loading. Data represent the mean ± SD; $n = 3$ biological replicates per condition per cell line.